Comparison between two iterative schemes for the 1D Marchenko equation

João Cândido Magalhães, Jörg Schleicher & Amélia Novais, University of Campinas (UNICAMP), and INCT-GP, Brazil

Abstract

Solving the 1D Marchenko equation by means of iterative schemes allows to obtain the redatumed Green's function at an arbtrary focusing position. We compare two algorithms proposed in the literature to achieve this goal. Our careful implementations have demonstrated that while kinematically equivalent, these algorithms lead not to fully identical results. While the older algorithm is somewhat faster, the newer one provides superior amplitudes and separate up and downgoing components of the recovered Green's function.

Introduction

The one dimensional Marchenko equation is a well-known integral equation that solves the inverse scattering problem for a constant background medium with some localized scattering region.

Rose (2002) developed an iterative way to construct a particular initial waveform that reduces to a δ at a particular time, called the focusing time. He also proved that by constructing this waveform we are solving the Marchenko equation.

Broggini and Snieder (2012) demonstrated that combining the solution of this scheme with its time-reversed version allows to obtain the redatumed Green's function at a focusing position. Wapenaar et al. (2013) extended this principle to three dimensions and derived, via Green's theorem, the coupled Marchenko equations, which constitute a relationship between the Green's function and the fundamental solutions of the inverse scattering problem. van der Neut et al. (2015) later developed an alternative iterative scheme to solve the coupled Marchenko equations. His scheme bears some similarity to Rose's iterative scheme.

In this paper, we present a derivation of the one dimensional coupled Marchenko equations and show a comparison between the two schemes.

Theory

The Marchenko Integral Equation is a relation that solves the perturbed Helmholtz equation, also known as time independent Schrödinger equation (Lamb, 1980), given by

$$\frac{d^2}{dx^2}\widehat{f}(x,\omega)+\left[\left(\frac{\omega}{c_0}\right)^2-\alpha(x)\right]\widehat{f}(x,\omega)=0\,. \qquad (1)$$

Here, $\widehat{f}(x,\omega)$ is the fundamental solution for this type of problem, and $\alpha(x)$ is the medium perturbation, also called the localized scattering potential.

It is well-known that a second-order differential equation like (1) has two fundamental solutions. For brevity purposes, here we consider only the fundamental solution consisting of a right-going waveform inciding from the left-hand side, crossing the scattering region in such a way that on its right-hand side only a δ-pulse propagates to the right. This fundamental solution can be represented in the time domain as

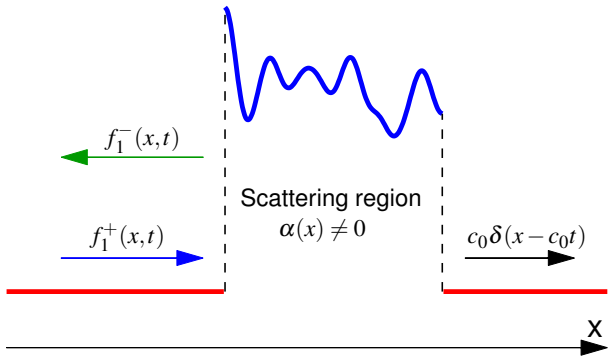

Figure 1: Right-going fundamental solution of equation (1). A wavefield $f_1^+(x,t)$ consisting of a δ-pulse and a coda incides from the left (blue arrow) on the localized scattering region ($\alpha(x)\neq 0$), producing a scattered wavefield $f_1^-(x,t)$ (green arrow) propagating to the left and a δ-pulse (black arrow) propagating to the right. All right-going scattered events produced by the incident δ-pulse are canceled by the coda.

Wapenaar et al. (2013) denominate the fundamental solution $f_1(x,t)$ focusing function, because to the right of the scattering region, it consists of a right-going δ-pulse only. For this reason, we can relate it with the Green's function $\mathscr{G}(x,\omega;x_s)$, i.e., the solution of

$$\frac{d^2}{dx^2}\widehat{\mathscr{G}}(x,\omega;x_s)+\frac{\omega^2}{c(x)^2}\widehat{\mathscr{G}}(x,\omega;x_s)=\delta(x-x_s)\,. \qquad (3)$$

Actually, since in a homogeneous 1D unbounded medium, the solution to equation (3) is (Bleistein et al., 2001)

$$\mathscr{G}(x,t;x_s)=\frac{c_0}{2}H(c_0t-|x-x_s|)\,, \qquad (4)$$

but we want to see a propagating unitary pulse, we consider a modified version of equation (3) with a time

derivative and a normalization applied to the source term, i.e.,

$$\frac{d^2}{dx^2}\widehat{G}(x,\omega;x_s)+\frac{\omega^2}{c(x)^2}\widehat{G}(x,\omega;x_s)=2i\frac{\omega}{c_0}\delta(x-x_s)\ , \qquad (5)$$

where

$$\widehat{G}=2i\frac{\omega}{c_0}\widehat{\mathscr{G}}\ . \qquad (6)$$

Next, we multiply equation (1) by $\widehat{G}(x,\omega;x_s)$, and equation (5) by $\widehat{f}_1(x,\omega)$ and subtract the results. We then integrate the differences from slightly beyond the source point x_s to slightly beyond the desired focusing point x_f and apply the 1D version of Green's theorem (see, e.g., Bleistein et al., 2001). In this way, we find

$$\lim_{\varepsilon\to 0^+}\Big|\left(\widehat{G}^+ + \widehat{G}^-\right)\frac{d}{dx}\left[\widehat{f}_1^{\,+}+\widehat{f}_1^{\,-}\right] - \left(\widehat{f}_1^{\,+}+\widehat{f}_1^{\,-}\right)\frac{d}{dx}\left[\widehat{G}^+ + \widehat{G}^-\right]\Big|_{x_s+\varepsilon}^{x_f+\varepsilon}=0\ , \qquad (7)$$

where we have assumed that the velocity distribution $c(x)$ in equation (3) equals the one in equation (1) within the interval (x_s,x_f) and that the velocity is constant in the small vicinities of size ε to the right of x_s and x_f. Moreover, we have written the involved wavefield as sums of their left-going (-) and right-going (+) components.

Using a high frequency approximation for both wavefields, we can show that at x_s and x_f,

$$\widehat{G}^-\frac{d}{dx}\widehat{f}_1^{\,-}\approx\ \widehat{f}_1^{\,-}\frac{d}{dx}\widehat{G}^-\quad\text{and}\quad\widehat{G}^+\frac{d}{dx}\widehat{f}_1^{\,+}\approx\ \widehat{f}_1^{\,+}\frac{d}{dx}\widehat{G}^+\ , \qquad (8)$$

$$\widehat{G}^-\frac{d}{dx}\widehat{f}_1^{\,+}\approx-\widehat{f}_1^{\,+}\frac{d}{dx}\widehat{G}^-\quad\text{and}\quad\widehat{G}^+\frac{d}{dx}\widehat{f}_1^{\,-}\approx-\widehat{f}_1^{\,-}\frac{d}{dx}\widehat{G}^+\ . \qquad (9)$$

Thus, in the limit of very small ε, equation (7) simplifies to

$$\lim_{\varepsilon\to 0^+}\left[\widehat{G}^+\frac{d}{dx}\widehat{f}_1^{\,-}+\widehat{G}^-\frac{d}{dx}\widehat{f}_1^{\,+}\right]\Big|_{x=x_f+\varepsilon} = -\lim_{\varepsilon\to 0^+}\left[\widehat{f}_1^{\,+}\frac{d}{dx}\widehat{G}^-+\widehat{f}_1^{\,-}\frac{d}{dx}\widehat{G}^+\right]\Big|_{x=x_s+\varepsilon}\ . \qquad (10)$$

Our fundamental solution $f_1(x,t)$ has to satisfy some convenient constraints. We require it to pass at focusing point x_f at $t=0$, which implies that it has to pass at x_s (the source injection position for $G(x,t;x_s)$) at $t=-t_f$, where t_f is the one-way traveltime between x_s and x_f. Moreover, beyond x_f, f_1^+ is given, by construction, by a δ-pulse and f_1^- vanishes. These requirements translate into the conditions

$$\frac{d}{dx}\widehat{f}_1^{\,-}(x_f+\varepsilon,\omega)=0\ , \qquad (11)$$

$$\frac{d}{dx}\widehat{f}_1^{\,+}(x_f+\varepsilon,\omega)=i\frac{\omega}{c_0}e^{i\omega\varepsilon/c_0}\ . \qquad (12)$$

Moreover, since the medium is assumed to be homogeneous to the left of x_s, the right-going part of G slightly to the right of x_s must still be equal to what it would be in a homogeneous medium. Thus, taking the derivative and Fourier Transform of equation (4) and making use of equation (6), we find

$$\frac{d}{dx}\widehat{G}^+(x_s+\varepsilon,w,x_s)=i\frac{\omega}{c_0}e^{i\omega\varepsilon/c_0}\ . \qquad (13)$$

Finally, the left-going part of the Green's function is related to the reflection response $R(x_s,t,x_s)$ of the medium. Taking the spatial derivative of its Fourier transform, we therefore have

$$\frac{d}{dx}\widehat{G}^-(x_s+\varepsilon,\omega,x_s)\approx-i\frac{\omega}{c_0}\widehat{R}(x_s+\varepsilon,\omega;x_s)\ , \qquad (14)$$

where $\widehat{R}(x,\omega;x_s)$ is the reflection response of the medium for the normalized source according to equation (5).

Substituting these boundary conditions in equation (10) and taking the limits results in

$$\widehat{G}^-(x_f,\omega;x_s)=\widehat{R}(x_s,\omega;x_s)\widehat{f}_1^{\,+}(x_s,\omega)-\widehat{f}_1^{\,-}(x_s,\omega)\ , \qquad (15)$$

$$G^-(x_f,t;x_s)=R(x_s,t;x_s)*f_1^+(x_s,t)-f_1^-(x_s,t)\ . \qquad (16)$$

The same procedure applied to the time reversed version of f_1, i.e., using the complex conjugate of equation (1), yields

$$\widehat{G}^+(x_f,\omega;x_s)=-\widehat{R}(x_s,\omega;x_s)\widehat{f}_1^{\,-*}(x_s,\omega)+\widehat{f}_1^{\,+*}(x_s,\omega)\ , \qquad (17)$$

$$G^+(x_f,t;x_s)=-R(x_s,t;x_s)*f_1^-(x_s,-t)+f_1^+(x_s,-t)\ . \qquad (18)$$

Expressions (15) and (17), or (16) and (18) in the time domain, are called the coupled Marchenko equations (Wapenaar et al., 2013).

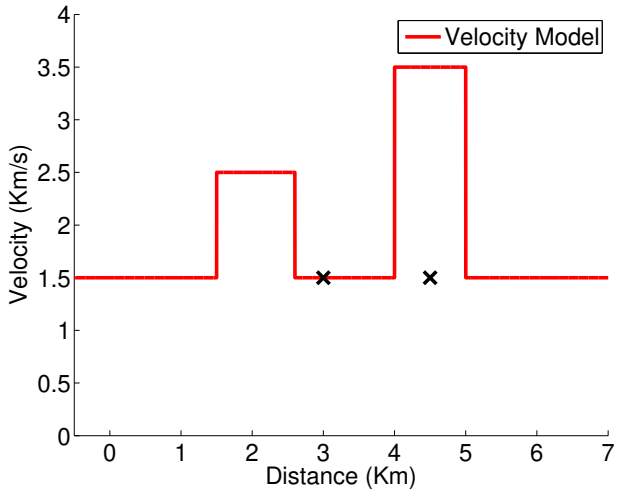

Figure 2: Velocity model. Markers denoted by $\times$ are the chosen focusing points.

Broggini and Snieder's method

On the basis of the work of Rose (2002), Broggini and Snieder (2012) developed an iterative scheme that focuses an initial pulse at a prescribed time t_f using data recorded with a zero-offset configuration. To graphically demonstrate the underlying operations, we use the model depicted in Figure 2 with the leftmost focusing point.

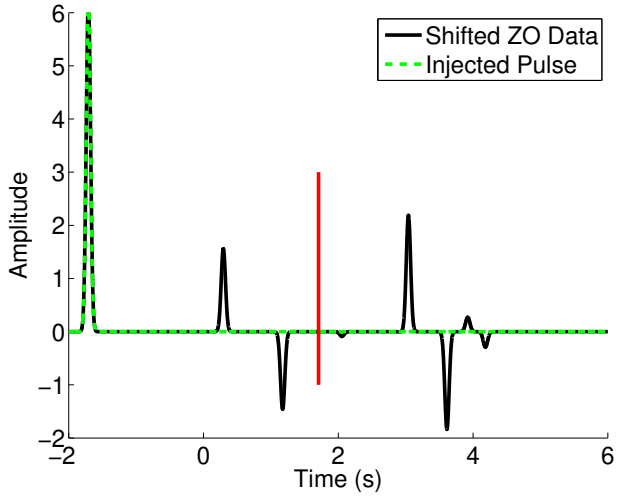

Figure 3: Broggini and Snieder's Algorithm: The Gaussian wavelet $Q^0(t) = Q(t)$ simulating a δ-pulse used at the first iteration (dashed green line) and the corresponding recorded seismogram $S^0(x_s,t;x_s)$ (solid black line).

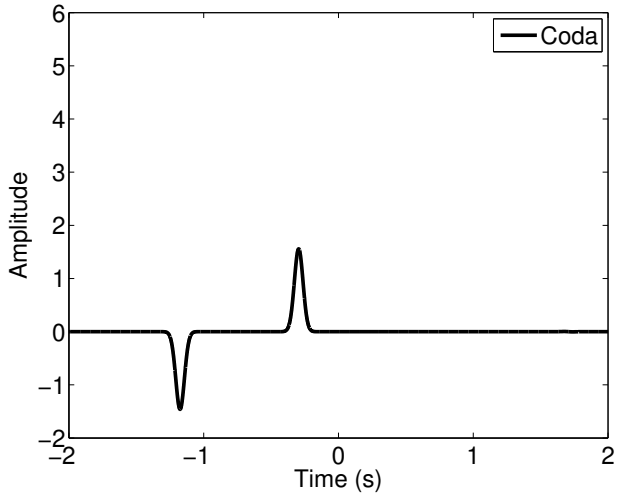

Figure 4: Broggini and Snieder's Algorithm: Time reversed and windowed reflection response at the first iteration, $coda^0(t)$, obtained according to equation (20).

The procedure proposed by Rose (2002) consists in first injecting at x_s a known pulse $Q^0(t) = q(t) \equiv \frac{d}{dt}\delta(t + t_f)\delta(x - x_s)$ shifted to $-t_f$ and record the medium response $S^0(x_s,t;x_s)$. Because the solution of the one dimensional wave equation integrates the initial wavelet (since the Green's function is a Heaviside function), by injecting $\frac{d}{dt}Q(t)$ the recorded wavefield will have the desired wavelet shape $Q(t)$. Second, to obtain the reflection response $R^0(x_s,t;x_s)$ simply take the difference between the recorded wavefield at x_s and the injected pulse,

$$R^0(x_s,t;x_s) = S^0(x_s,t;x_s) - Q^0(t)\ . \tag{19}$$

(Figure 3) shows this result for a model with two high-velocity zones between x_s and x_f. $R^0(x_s,t;x_s)$ can be replaced by a recorded reflection response, $R(x_s,t;x_s)$, if available.

The third step consists of applying a window operator $H(t_f - t)$ to the reflection response $R^0(x_s,t;x_s)$ and reversing it in time. This time reversed version, called coda (Figure 4), is given by

$$coda^0(t) = R^0(x_s,-t;x_s)H(t_f + t)\ . \tag{20}$$

Next, the injected pulse is updated by taking the difference between the initial wavelet $Q^0(t)$ and the coda $coda^0(t)$ to produce the new wavelet $Q^1(t)$ (Figure 5). The procedure starts then over by injecting $\frac{d}{dt}Q^1(t)$, recording the new response $R^1(x_s,t;x_s)$, and calculating the new $coda^1(t)$. At each iteration, $Q^k(t)$ is obtained by subtracting the coda from Q^0. The process continues iteratively k times until it reaches convergence to obtain $Q^k(t)$.

Broggini and Snieder (2012) showed that $G(x_f,w;x_s)$ can be obtained by convolving the original seismic reflection response $R(x_s,t;x_s)$ at x_s with the injected wavelet $Q(t)$ as described above, i.e., after k iterations, $u(x_s,t) = R(x_s,t;x_s) *_t Q^k(t)$ (Figure 6), and adding its time reversed version $u(x_s,-t)$ (Figure 7a). Figure 6 shows the result

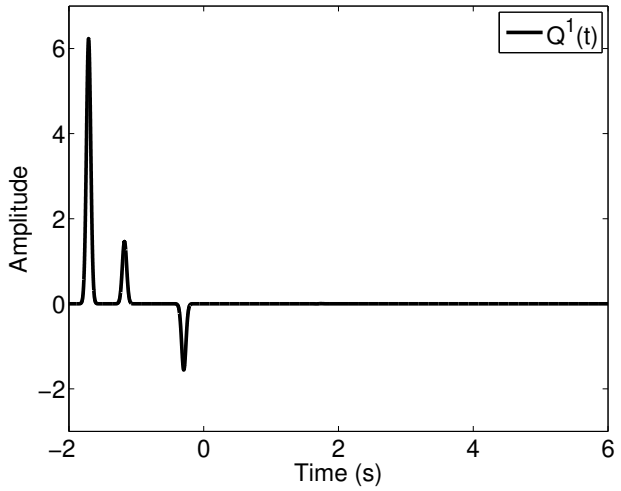

Figure 5: Wavelet $Q^1(t)$ after first iteration update.

of this procedure after four iterations. The algorithm is summarized in Table 1.

Note that the redatumed Green's function in Figure 7a has a higher amplitude than the reference solution calculated with an FD scheme. This is due to the transmission coefficients that exists between x_s and x_f that are not captured in the solution. Brackenhoff (2016) addresses this problem in his work.

van der Neut's method

For the coupled Marchenko equations, van der Neut et al. (2015) developed the following iterative scheme: First, think of f_1^+ as composed of a initial unitary direct pulse f_d and a following coda corresponding to equation (2), i.e.,

$$f_1^+ = f_d + f_{coda}\ . \tag{21}$$

Note again that the designed focusing function is subject to some constraints: f_d has to pass at x_s at a specified

Broggini and Snieder's Algorithm

1. $k \leftarrow 0$
2. $Q^k(t) \leftarrow \delta(t+t_f)$
3. Inject Q^k and record S^k at x_s
4. $R^k \leftarrow S^k - Q^k$
5. $coda^k \leftarrow R^k(-t)H(t_f+t)$
6. $Q^{k+1}(t) \leftarrow Q^0 - coda^k$
7. $k \leftarrow k+1$;
8. If Q^k does not satisfy convergence criteria: Goto step 3
9. After convergence: Inject Q^k and record $u(t) = S^k(t)$
10. $G^k \leftarrow u(t) + u(-t)$

Table 1: Broggini and Snieder's Algorithm.

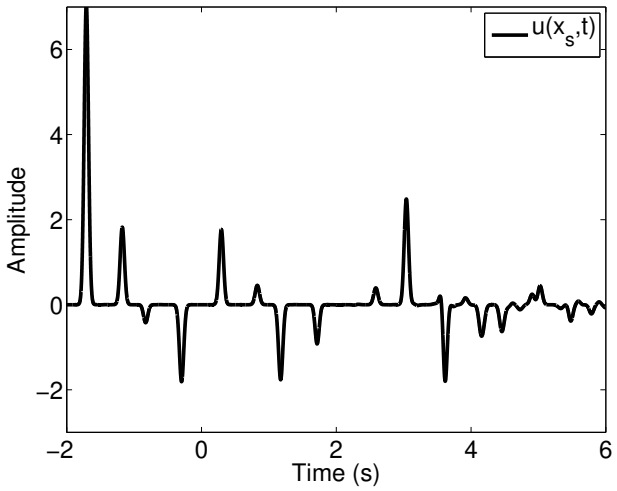

Figure 6: Seismogram recorded after 4 interations, i.e., injecting $\frac{d}{dt}Q^3(t)$.

focusing time $-t_f$ so as to reach the focusing point x_f at $t = 0$. Hence, without any knowledge of the velocity model, the obtained Green's function will be simulated at an unknown position.

Consistent with the boundary conditions, design a window operator $\Theta = H(tf - |t|)$, that preserves the field between $-t_f$ and t_f, and zeroes the field outside this interval. Windowing f_1^-, f_1^+, and G results in

$$\Theta\{G\} = 0\ , \tag{22}$$

$$\Theta\{f_1^+\} = f_{coda}\ , \tag{23}$$

$$\Theta\{f_1^-\} = f_1^-\ . \tag{24}$$

van der Neut's Algorithm

1. $f_d(t) \leftarrow \delta(t+t_f)$
2. $k \leftarrow 0$
3. $f_{coda}^k \leftarrow 0$
4. $f_1^{+k} = f_d + f_{coda}^k$
5. $f_1^{-k} \leftarrow \Theta\{R * f_1^{+k}\}$
6. $f_{coda}^{+(k+1)}(x_s,-t) \leftarrow \Theta\{R * f_1^{-k}\}$
7. $k \leftarrow k+1$;
8. If f_{coda}^{+k} does not satisfy convergence criteria: Goto step 4
9. After convergence: $G^{-k} \leftarrow R(t) * f_1^{+k}(t) - f_1^{-k}(t)$
10. $G^{+k} \leftarrow -R(t) * f_1^{-k}(-t) + f_1^{+k}(-t)$
11. $G^k \leftarrow G^{+k} + G^{-k}$

Table 2: van der Neut's Algorithm.

It is important to recognize that there is no field registered before t_f at x_s because the Green's function localized at x_f is causal. Thus, masking the Green's function with Θ gives zero. On the other hand, the leftward propagating part of f^1 exists only within the time window between $-t_f$ and t_f, so that it is not affected by the masking.

The masking of f_1^+ in the prescribed two-way traveltime window ($-t_f$ to t_f) is done in such a way that the direct field f_d is removed, but all primaries and multiples that will possibly arrive at x_s are preserved. Using this window operator on the time domain coupled Marchenko equations yields

$$\Theta\{R(x_s,t;x_s) * f_1^+(x_s,t)\} = f_1^-(x_s,t)\ , \tag{25}$$

$$\Theta\{R(x_s,t;x_s) * f_1^-(x_s,-t)\} = f_{coda}^+(x_s,-t)\ . \tag{26}$$

The algorithm starts by setting $f_{coda}^0 = 0$ and $f_d^0 = \delta(c_0(t+tf) - |x - x_s|)$ in the first iteration. The use of these initial values in equation (25) yields f_1^{-0}, which, upon substitution in equation (26), provides f_{coda}^1. This iterative process can be repeated until it meets some convergence criteria. Upon reaching convergence, G^+ and G^- are calculated by equations (16) and (18). Figure 7b shows the complete Green's function obtained with this iterative scheme. The algorithm is summarized in Table 2.

Numerical examples

Our numerical tests performed with the above described algorithms demonstrated that the mentioned amplitude discrepancy shown in Figure 7a between the result of Broggini and Snieder's algorithm (green dashed lines) and the modeled Green's function (solid black line) is intrinsic to their procedure. At the second focusing point in the model in Figure 2, which is not located in a region with $c = c_0$, the effect is even stronger (see Figure 8a). Brackenhoff (2016)

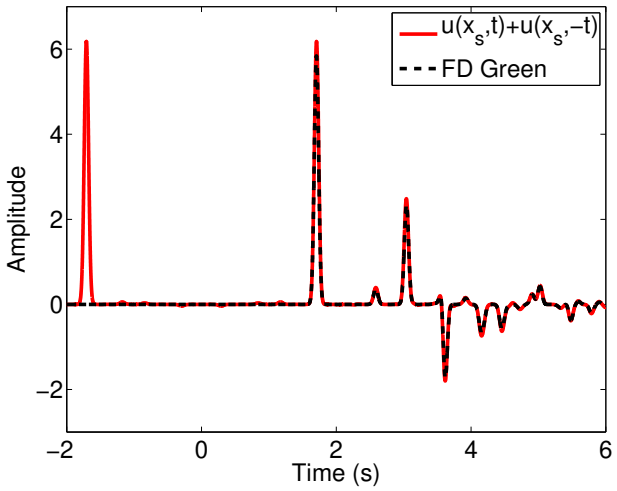

(a) Numerical result using Broggini and Snieder's iterative algorithm.

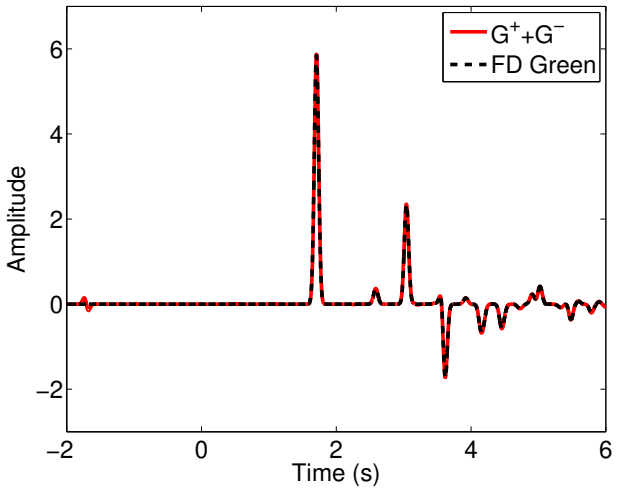

(b) Numerical result using van der Neut's iterative algorithm based on the coupled Marchenko equations.

Figure 7: Results for the first focusing time $t_f = 1.7$ s corresponding to $x_f = 3$ km (left $\times$ in Figure 2).

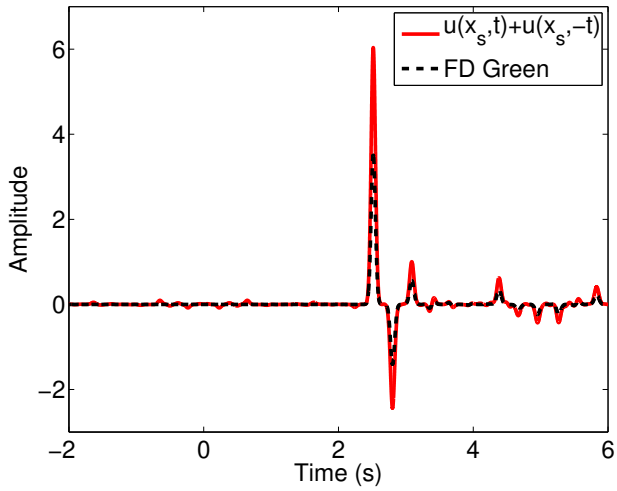

(a) Numerical result using Broggini and Snieder's iterative algorithm.

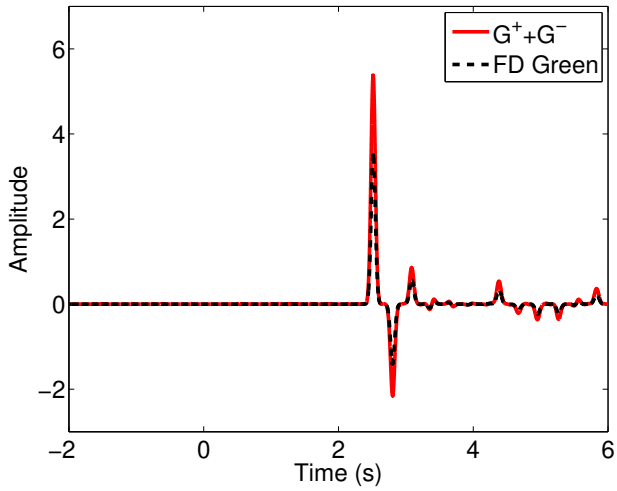

(b) Numerical result using van der Neut's iterative algorithm.

Figure 8: Results for the second focusing time $t_f = 2.5$ s corresponding to $x_f = 4.5$ km (right $\times$ in Figure 2).

explains this effect by incorrectly treated transmission coefficients by these algorithms.

The agreement in Figures 7b and 8b between the recovered Green's functions using van der Neut's algorithm (solid red lines) and the modeled versions (dashed black lines) is much better. This shows that the theoretical derivations are consistent and that under the ideal conditions simulated here, the true Green's function for a source at the focusing point is recovered by this algorithm.

Conclusions

In this work, we have investigated two well-known iterative algorithms for solving the 1D Marchenko equation to construct the Green's function for a point source at an arbitrary focusing point. Our careful implementations have demonstrated that while kinematically equivalent, these algorithms lead not to fully identical results. The algorithm of Broggini and Snieder (2012) is somewhat faster than the one of van der Neut et al. (2015), because the latter needs two wavefield propagations per iteration instead of a single one. However, it allows only the construction of the complete Green's function, where van der Neut's algorithm allows for the separate calculation of the up and downgoing components.

Acknowledgments

This work was kindly supported by the Brazilian research council CNPq, as well as by Petrobras through the Human Resource Project PRH-PB230 and a research project on seismic interferometry.

References

Bleistein, N., J. K. Cohen, and J. W. Stockwell Jr., 2001, Mathematics of multidimensional seismic imaging, migration, and inversion: Springer.

Brackenhoff, J., 2016, Rescaling of incorrect source strength using Marchenko redatuming: Master's thesis, Delft University of Technology.

Broggini, F., and R. Snieder, 2012, Connection of scattering princples: A visual and mathematical tour: European Journal of Physics, **33**.

Lamb, G. L., 1980, Elements of soliton theory: Willey & Sons.

Rose, J. H., 2002, Single-sided autofocusing of sound in layered materials: Inverse Problems, **18**.

van der Neut, J., I. Vasconscelos, and K. Wapenaar, 2015, On Green's function retrieval by iterative substitution of the coupled Marchenko equations: Geophysical Journal International.

Wapenaar, K., F. Broggini, E. Slob, and R. Snieder, 2013, Three-dimensional single-sided Marchenko inverse scattering, data-driven focusing, Green's function retrieval, and their mutual relations: Physical Review Letters, **110**.